Ion flux, transmembrane potential, and osmotic stabilization: A new electrophysiological dynamic model for Eukaryotic cells

Clair Poignard, Aude Silve, Frederic Campion, Lluis M. Mir, Olivier Saut, Laurent Schwartz

INSTITUT NATIONAL DE RECHERCHE EN INFORMATIQUE ET EN AUTOMATIQUE

Ion flux, transmembrane potential, and osmotic stabilization: A new electrophysiological dynamic model for Eukaryotic cells

Clair Poignard — Aude Silve — Frederic Campion — Lluis M. Mir — Olivier Saut — Laurent Schwartz

N° 7269

Avril 2010

Thème NUM

ISSN 0249-6399 ISRN INRIA/RR--7269--FR+ENG

INSTITUT NATIONAL
DE RECHERCHE
EN INFORMATIQUE
ET EN AUTOMATIQUE

INRIA

centre de recherche
BORDEAUX - SUD OUEST

Ion flux, transmembrane potential, and osmotic stabilization: A new electrophysiological dynamic model for Eukaryotic cells

Clair Poignard* , Aude Silve† , Frederic Campion‡ , Lluis M. Mir§, Olivier Saut¶ , Laurent Schwartz‖

Thème NUM — Systèmes numériques
Équipes-Projets MC2

Rapport de recherche n° 7269 — Avril 2010 — 20 pages

Abstract: Survival of mammalian cells is achieved by tight control of cell volume while transmembrane potential is known to control many cellular functions since the seminal work of Hodgkin and Huxley. Regulation of cell volume and transmembrane potential have a wide range of implications in physiology, from neurological and cardiac disorders to cancer and muscle fatigue. Therefore understanding the relationship between transmembrane potential, ion fluxes, and cell volume regulation has become of great interest. In this paper we derive a system of differential equations that links transmembrane potential, ionic concentrations, and cell volume. This model demonstrates that volume stabilization occurs within minutes of changes in extracellular osmotic pressure. We infer a straightforward relationship between transmembrane potential and cell volume. Our model is a generalization of previous models in which either cell volume was constant or osmotic regulation instantaneous. When the extracellular osmotic pressure is constant, the cell volume varies as a function of transmembrane potential and ions fluxes thus providing an implicit link between transmembrane potential and cell growth. Numerical simulations of the model provide results that are consistent with experimental data in terms of time-related changes in cell volume and dynamics of the phenomena.

Key-words: Electric potential – Cell volume regulation – Ion concentration – Membrane permeability – Osmotic equilibrium

* INRIA Bordeaux-Sud-Ouest, Institut de Mathématiques de Bordeaux, CNRS UMR 5251 & Université de Bordeaux1, 351 cours de la Libération, 33405 Talence Cedex, France
† CNRS, UMR 8203, Laboratory of Vectorology and Anticancer Therapies, Institut Gustave Roussy& Université Paris-Sud. 114, rue Edouard Vaillant, 94805 Villejuif, France.
‡ The Copenhagen Muscle Research Centre, Rigshospitalet, 2200 Copenhagen N, Denmark.
§ CNRS, UMR 8203, Laboratory of Vectorology and Anticancer Therapies, Institut Gustave Roussy& Université Paris-Sud. 114, rue Edouard Vaillant, 94805 Villejuif, France.
¶ INRIA Bordeaux-Sud-Ouest, Institut de Mathématiques de Bordeaux, CNRS UMR 5251 & Université de Bordeaux1, 351 cours de la Libération, 33405 Talence Cedex, France
‖ Service de Radiothérapie, Hôpital Universitaire Pitié-Salpétrière, 75013 Paris, France & LIX, Laboratoire d'Informatique, Ecole Polytechnique

Centre de recherche INRIA Bordeaux – Sud Ouest
Domaine Universitaire - 351, cours de la Libération 33405 Talence Cedex
Téléphone : +33 5 40 00 69 00

Flux ioniques, potentiel transmembranaire et stabilisation osmotique: un modèle dynamique d'électrophysiologie pour les cellules eucaryotes

Résumé : Pas de résumé

Mots-clés : Potentiel Electrique de Membrane – Régulation du volume cellulaire – Concentration ionique – Perméabilité membranaire – Equilibre osmotique

Contents

1 Introduction

Cell volume and resting transmembrane potential constitute two fundamental parameters of cell life. A cell contains inside its cytoplasm substances such as DNA, amino acids, ions like K^+ or Na^+ and sugar, which are essential to its survival. This synthetic process favors swelling of the cell [17], since the membrane permeability is very low. Without volume changes, the pressure created by the osmolarity difference between the outer medium and the cytoplasm could reach an atmosphere [1, 7], which is much larger than the maximal pressure that the cell membrane can withstand. Whereas plasmalemma of bacteria are protected by a thick peptidoglycan layer that can support such pressures, Eukaryotic cells have no wall and therefore must adjust their osmolarity by transferring ions and water accross their membrane. Over many years, it became clear that the osmotic stabilization of living Eukaryotic cells was related to the active transport of Na^+ out of and K^+ into the cell [9, 16, 11, 12]. These ion fluxes create a potential difference across the membrane that changes the value of the transmembrane potential. Therefore the cell volume regulation and the transmembrane potential are intrinsically correlated.

Based on the extensive review of Fraser and Huang [7, 8], all theoretical models (to our knowledge) describing the behavior of the transmembrane potential, of the ionic fluxes, and of the cell volume consider that the water flux across the membrane is instantaneous. Therefore an osmotic equilibrium of the cell is constantly required [1, 5, 7]. However, such a requirement does not explain the delay in the experiments reported by Rouzaire-Dubois *et al.* [21, 4, 22] in the osmotic stabilization of the cell, when a high osmotic stress is imposed. Actually, when the ionic fluxes across the membrane are small, the osmotic equilibrium can be considered constant as supposed by Fraser and Huang [7, 8] or Armstrong [1] for instance. However should the cell be subjected to a large osmotic stress, then water flux across the membrane must be accounted for.

In this paper we aim to clarify the relationship between cell volume, transmembrane potential and ion fluxes. More precisely, we aim at providing a new electrophysiological model of the cell in order to dynamically link the cell volume, the ionic concentrations, and the transmembrane potential by considering the water flux accross the membrane. Our model is a generalization of the previous models in the sense that it describes the models of Jakobsson [14], Armstrong [1], Fraser and Huang [7] or Endresen *et al.* [5] under their respective restrictive hypotheses. Our goal is also to propose an explanation for the results presented by Rouzaire-Dubois *et al.*[21, 4, 22].

In order to derive our model, we consider *in vitro* cell cultures and more precisely spherical cells in suspension. The extracellular ionic concentrations are supposed constant and the cell volume regulation occurs homothetically (*i.e.* equivalently in all directions). These assumptions are justified for *in vitro* experiments since the volume of the ambient medium is much larger than the cell volume and since no mechanical stress is imposed to the cell. Experimentally, the osmotic equilibrium is not enforced instantaneously contrary to the assumptions of the models of Jakobsson [14], Armstrong [1], Fraser and Huang [7], and Endresen *et al.* [5]. The main feature of the present model is the time-dependent variability of the cell volume $\mathfrak{v}_i$ since water molecules slowly diffuse across the cell membrane. Our model leads to an implicit dynamic link (the time derivative of the cell volume is a function of the transmembrane potential)

between the cell volume, the transmembrane voltage potential, and the ionic concentrations. In the case of spherical cell, we explicit this link and perform numerical simulations.

Such a dynamic relationship between the cell volume and the transmembrane potential has not yet, to the best of our knowledge, been investigated. Three main results are presented in this paper: the new cell model (which takes the water diffusion into account), the explicit link between the cell volume and the transmembrane potential, and the explicit expression of the potential in terms of ionic concentrations.

For the sake of simplicity, we omit the contribution of active channels such as Na^+/K^+ pumps and voltage-dependent ionic channels. These more accurate descriptions of the ionic fluxes can be added to our model with a very slight modification and without affecting the modelling principle. Our model can already provide some insight in specific mechanisms such as regulation of muscle fatigue. Osmotically induced cell swelling has been observed during muscle contraction [23], while muscle fatigue is associated with membrane depolarization [15, 2]. Our model represents an integration of these results.

In section 2, we derive the ordinary differential equations that describe the transmembrane potential in terms of ionic concentrations and cell volume. Section 3 is devoted to the numerical simulations of the equations. In Section 4, experiments that corroborate the numerical results are presented and we concluded by discussion.

2 The transmembrane potential

According to its phospholipid composition, the cell membrane is a resistive medium with a capacitance C_m in F.m^{-2}. We denote by $\mathfrak{S}_{ions}$ the group of ionic species. For our numerical simulations, $\mathfrak{S}_{ions}$ is $\{Na^+, Cl^-, K^+, X^-\}$, where X^- denotes the whole of the other ions that are considered non-permeant. This set is globally negatively charged on account of the excess Na^+ and K^+ inside the cell, and the mean charge valency of X^- equals -1.6 according to Fraser and Huang [7] and the references therein.

The membrane is sprinkled over with ionic channels, across which ionic exchanges occur. The valency of the ions S is denoted by z_S, and the constant P_S denotes the membrane permeability to the species S. In the following, R and F denote respectively the gas constant and the Faraday constant, and the temperature is denoted by T. Glossary of Table 1 summarizes the notations used in the paper.

2.1 Ion flux through channels

According to the literature [1, 3, 5, 13], the ionic fluxes depend on the transmembrane potential V_m. We use the convention $V_m = V_i - V_o$, where the indices i and o hold respectively for inner and outer part of the membrane. The ion flux equation previously described in 1943 by Goldman [9], and modified in 1949 by Hodgkin and Katz [11], is based on a Gas-Law model. It is precisely described in the book of Malmivuo and Plonsey [19], and in the article of Endresen *et al.* [5] (see also Armstrong [1]). According to these models, the current I_S of the

Table 1: Glossary

R	gas constant
F	Faraday constant
T	temperature
c	equal to $F/(2RT)$
$\mathfrak{v}_i$	cell volume
$\mathscr{A}(\Gamma)$	membrane area
C_m	cell capacitance
V_m	transmembrane potential
τ_w	membrane penetrability to water
Θ_w	equal to $RT\tau_w$
$\mathfrak{S}_{ions}$	group of all the considered ionic species
S	specific ionic species belonging to the group $\mathfrak{S}_{ions}$
$[S]_e$	extracellular concentration of ions S
$[S]_i$	cell concentration of ions S
n_S^i	amount of substance of ions S in the cell
P_S	membrane permeability to ions S
z_S	valency of S
I_S	current due to the fluxes of ions S
g_S	conductance for ions S
V_S	Nernst equilibrium potential of the ions S
Σ_e	total sum of outer concentrations
Σ_i	total sum of inner concentrations

permeant ion S equals:

$$I_S = \frac{1}{2} z_S P_S F \left([S]_i e^{z_S c V_m} - [S]_e e^{-z_S c V_m} \right),$$

where $c = F/(2RT)$. The Nernst equilibrium potential V_S of the species S is the potential such that I_S vanishes:

$$V_S = \frac{1}{2cz_S} \log \left(\frac{[S]_e}{[S]_i} \right), \tag{1}$$

Let g_S be the membrane conductance for the species S defined by

$$g_S = P_S z_S^2 c F \sqrt{[S]_e [S]_i}, \tag{2}$$

we therefore infer

$$I_S = g_S \frac{\sinh(z_S c (V_m - V_S))}{z_S c}. \tag{3}$$

When $z_S c(V_m - V_S)$ is small compared to 1, equation (3) leads to the linear equation

$$I_S = g_S (V_m - V_S). \tag{4}$$

2.2 Evolution of the ionic concentrations

The global amount of ions driven by the total current of ions $S \in \mathfrak{S}_{ions}$ across the membrane Γ equals

$$\frac{\mathrm{d}n_S^i}{\mathrm{d}t} = -\frac{\mathscr{A}(\Gamma)}{z_S F} I_S, \tag{5}$$

where $\mathscr{A}(\Gamma)$ denotes the membrane surface area.

2.3 Osmolarity

We denote by Σ_e and Σ_i the respective sums of the outer and inner concentrations

$$\Sigma_e = \sum_{S \in \mathfrak{S}_{ions}} [S]_e, \quad \Sigma_i = \sum_{S \in \mathfrak{S}_{ions}} n_S^i / \mathfrak{v}_i.$$

Since the water is incompressible, we suppose that the change of the cell volume is described by the rate of flow of water across the membrane. Let τ_w be the water membrane penetrability[1] in s.m^{-1} in S.I. units. We denote by Θ_w the following coefficient

$$\Theta_w = RT\tau_w.$$

According to the Landahl model [16] we infer

$$\frac{\mathrm{d}\mathfrak{v}_i}{\mathrm{d}t} = -\Theta_w \mathscr{A}(\Gamma)(\Sigma_e - \Sigma_i), \tag{6}$$

[1]The parameter τ_w is a penetrability hence it is homogeneous to the inverse of a velocity. We refer to Landalh [16] for more precision.

Recently, Hernández and Cristina [10], or Mathai *et al.* [20] replaced Θ_w by the product of the membrane permeability P_w by the partial molar volume of water $\mathscr{V}_w$. Therefore the coefficients τ_w and P_w are linked by the following equality:

$$\tau_w = \frac{P_w \mathscr{V}_w}{RT}.$$

Remark 2.1. *In many models [1, 5, 7, 19], the plasma membrane cannot support a pressure difference. Therefore osmotic equilibrium is required at any time*

$$\Sigma_e = \Sigma_i, \quad \textit{which leads to} \quad \mathfrak{v}_i = \frac{1}{\Sigma_e} \sum_{S \in \mathfrak{S}_{ions}} n_i^S.$$

This equality enforces the volume to change instantaneously when the osmotic equilibrium is modified. However, the cell volume is adjusted by the diffusion of water molecules across the membrane. This phenomenon takes time and is described by the model of Landahl [16], which is based on Fick's law type model to describe the diffusion of water molecules through the membrane.

Remark 2.2. *Note that Mathai et al. [20] write the volume change* (6) *in a different way. Let R_{vol} be the ratio of the volume $\mathfrak{v}_i$ at the time t divided by the initial volume $\mathfrak{v}_i^0$, and denote by Σ_i^0 the sum of the initial inner concentrations. Mathai et al. suppose that cell membrane is perfectly non permeant. Since no exchange occurs inner and outer amounts of substance of the ionic species are constant. Therefore*

$$\Sigma_i = \Pi_i^0 / R_{vol},$$

and we infer the Mathai et al. equation:

$$\frac{\mathrm{d}R_{vol}}{\mathrm{d}t} = -\Theta_w \frac{\mathscr{A}(\Gamma)}{\mathfrak{v}_i^0} \left(\Sigma_e - \frac{\Pi_i^0}{R_{vol}} \right). \tag{7}$$

However, we emphasize that we cannot consider the inner amounts of substance constant since the ionic fluxes drive ions across the membrane. Therefore equation (6) *must be used. Observe that equation* (6) *leads to* (7) *by considering that no ionic flux across the membrane occurs.*

2.4 Equations for the transmembrane potential

Our model links the transmembrane potential, the cell volume, and the ionic concentrations inside and outside the cell. The unknown quantities are the transmembrane potential V_m, the cell volume $\mathfrak{v}_i$, and the amount in the cell of substances n_S^i of the ions $S \in \mathfrak{S}_{ions}$. We obtain a system of ordinary differential equations. This system is very similar to the models of Endresen *et al.* [5] and Armstrong [1]. The main difference consists in the fact that the cell volume evolution is governed by an ordinary differential equation while Endresen *et al.* and Armstrong *et al.* required osmotic equilibrium at any time. Using the

Kirchoff law and the above equalities we infer

$$C_m \frac{\mathrm{d}V_m}{\mathrm{d}t} + \sum_{S\in\mathfrak{S}_{ions}} I_S = 0, \tag{8a}$$

$$I_S = g_S \frac{\sinh(z_S c(V_m - V_S))}{z_S c}, \quad \text{for } S \in \mathfrak{S}_{ions}, \tag{8b}$$

$$\frac{\mathrm{d}n_S^i}{\mathrm{d}t} = -\frac{\mathscr{A}(\Gamma)}{z_S F} I_S, \tag{8c}$$

$$\frac{\mathrm{d}\mathfrak{v}_i}{\mathrm{d}t} = -\Theta_w \mathscr{A}(\Gamma)(\Sigma_e - \Sigma_i), \tag{8d}$$

where

$$\begin{cases} [S]_i = n_S^i/\mathfrak{v}_i, \quad V_S = \dfrac{1}{2z_S c}\log\left([S]_e/[S]_i\right), \quad g_S = z_S^2 P_S c F\sqrt{[S]_e n_S^i/\mathfrak{v}_i}, \\ \Sigma_e = \sum_{S\in\mathfrak{S}_{ions}}[S]_e, \quad \Sigma_i = \sum_{S\in\mathfrak{S}_{ions}}[S]_i. \end{cases} \tag{8e}$$

For the linearized model we replace (8b) by

$$I_S = g_S(V_m - V_S). \tag{9}$$

The novelty of the model consists in equation (8d), which describes the evolution of the cell volume. To solve problem (8), initial conditions are chosen for V_m, $\mathfrak{v}_i$, and concentrations n_S^i.

2.5 Explicit link between the cell radius and the potential

Problem (8) provides an implicit link between the cell volume and the transmembrane potential through the ionic concentrations and the ionic fluxes. The aim of the paragraph is to write explicitly this link. Equation (8d) can be rewritten as follows

$$\frac{1}{\Theta_w}\frac{\mathfrak{v}_i}{\mathscr{A}(\Gamma)}\frac{\mathrm{d}\mathfrak{v}_i}{\mathrm{d}t} = -\Sigma_e\mathfrak{v}_i + \sum_{S\in\mathfrak{S}} n_S^i.$$

Differenciating the above equality and using equation (8c) leads to

$$\frac{1}{\Theta_w}\frac{\mathrm{d}}{\mathrm{d}t}\left(\frac{\mathfrak{v}_i}{\mathscr{A}(\Gamma)}\frac{\mathrm{d}\mathfrak{v}_i}{\mathrm{d}t}\right) = -\Sigma_e\frac{\mathrm{d}\mathfrak{v}_i}{\mathrm{d}t} - \frac{\mathscr{A}(\Gamma)}{F}\sum_{S\in\mathfrak{S}}\frac{1}{z_S}I_S.$$

Considering the linearized model for the ionic fluxes we therefore infer the explicit link between the shape of the cell and the transmembrane potential:

$$\frac{1}{\Theta_w}\frac{\mathrm{d}}{\mathrm{d}t}\left(\frac{\mathfrak{v}_i}{\mathscr{A}(\Gamma)}\frac{\mathrm{d}\mathfrak{v}_i}{\mathrm{d}t}\right) = -\Sigma_e\frac{\mathrm{d}\mathfrak{v}_i}{\mathrm{d}t} - \frac{\mathscr{A}(\Gamma)}{F}\sum_{S\in\mathfrak{S}}\frac{g_S}{z_S}(V_m - V_S). \tag{10}$$

Observe that the above equation involves both cell volume and membrane area. To uniquely determine the shape of the cell it is necessary to add a law on the membrane surface. However, in the experiments, the cells in suspension are almost spherical and therefore the geometry is entirely determined by the cell radius. The next paragraph is devoted to give the explicit link between the transmembrane potential and the cell radius.

2.5.a The case of spherical cells

Let us now consider spherical cells. Equation (8d) leads to the following equation on the cell radius r:

$$\frac{1}{\Theta_w}\frac{\mathrm{d}r}{\mathrm{d}t} = -\left(\Sigma_e - \sum_{S\in\mathfrak{S}} \frac{n_S^i}{4\pi r^3/3}\right).$$

Using equation (8c) with the linearized model of the ionic fluxes, and by differenciation we obtain a non-linear differential equation on r:

$$\frac{1}{\Theta_w}\frac{1}{3r^2}\frac{\mathrm{d}}{\mathrm{d}t}\left(r^3\frac{\mathrm{d}r}{\mathrm{d}t}\right) = -\Sigma_e\frac{\mathrm{d}r}{\mathrm{d}t} - \sum_{S\in\mathfrak{S}_{ions}} \frac{g_S}{z_S F}(V_m - V_S). \tag{11a}$$

The initial conditions are then :

$$r|_{t=0} = r_0, \quad \left.\frac{\mathrm{d}r}{\mathrm{d}t}\right|_{t=0} = -\Theta_w(\Sigma_e - \Sigma_i^0). \tag{11b}$$

Denote by V_m^{rest} the resting transmembrane potential defined such that:

$$\sum_{S\in\mathfrak{S}_{ions}} \frac{g_S}{z_S}(V_m^{rest} - V_S) = 0.$$

If the cell is initially in osmotic equilibrium and if V_m equals V_m^{rest} then equation (11) shows that r remains at its initial value. However, a slight change in the value of V_m leads to an increase (or a decrease) of the cell radius.

2.6 Explicit formula for the transmembrane potential.

It is interesting to obtain an explicit expression of the transmembrane potential in terms of the ionic concentrations. This can be achieved by assuming that the cell shape does not change. Actually if the cell volume $\mathfrak{v}_i$ and the membrane area $\mathscr{A}(\Gamma)$ are constant –*i.e.* the osmotic equilibrium is reached– then using equality (8c), the equation (8a) writes

$$C_m\frac{\mathrm{d}V_m}{\mathrm{d}t} = \frac{\mathfrak{v}_i}{\mathscr{A}(\Gamma)}F\sum_{S\in\mathfrak{S}} z_S\frac{\mathrm{d}[S]_i}{\mathrm{d}t}.$$

Denoting by V_m^0 and $[S]_i^0$, the initial potential and inner concentrations respectively, we infer the explicit formula for the potential in terms of the inner concentrations at each time t:

$$\left(V_m - V_m^0\right) = \frac{\mathfrak{v}_i}{\mathscr{A}(\Gamma)}\frac{F}{C_m}\sum_{S\in\mathfrak{S}} z_S([S]_i - [S]_i^0). \tag{12}$$

Define the initial potential by

$$V_m^0 = \frac{\mathfrak{v}_i}{\mathscr{A}(\Gamma)}\frac{F}{C_m}\sum_{S\in\mathfrak{S}} z_S[S]_i^0. \tag{13}$$

Then, the following formula, that is similar to the "Charge Difference" equation of Fraser and Huang holds

$$V_m = \frac{\mathfrak{v}_i}{\mathscr{A}(\Gamma)} \frac{F}{C_m} \sum_{S \in \mathfrak{S}} z_S [S]_i.$$

Observe that the factor $\mathfrak{v}_i/\mathscr{A}(\Gamma)$ ensures the dimensional consistency of the previous equality. It is striking that equation (12) involves only the inner concentrations, while the concentrations of the exterior solution is expected to have an influence on the potential. This is hidden behind the hypothesis that the outer concentrations are constant, and by supposing that this equality (13) holds at the initial time. Actually, if the outer concentrations change, using the mass conservation law, we would have:

$$\frac{\mathrm{d}n_S^e}{\mathrm{d}t} = -\frac{\mathrm{d}n_S^i}{\mathrm{d}t}.$$

Therefore the expression (12) of the potential would be:

$$\big(V_m - V_m^0\big) = \frac{F}{2C_m} \frac{\mathfrak{v}_i}{\mathscr{A}(\Gamma)} \sum_{S \in \mathfrak{S}} z_S \big(([S]_i - [S]_e) - ([S]_i^0 - [S]_e^0)\big), \qquad (14)$$

and then supposing that

$$V_m^0 = \frac{F}{2C_m} \frac{\mathfrak{v}_i}{\mathscr{A}(\Gamma)} \sum_{S \in \mathfrak{S}} z_S ([S]_i^0 - [S]_e^0),$$

we would have

$$V_m = \frac{F}{2C_m} \frac{\mathfrak{v}_i}{\mathscr{A}(\Gamma)} \sum_{S \in \mathfrak{S}} z_S ([S]_i - [S]_e).$$

This formula is exactly the Endresen *et al.* formula (63) of [5]: just replace the factor $C_m \mathscr{A}(\Gamma)$ by the factor C of [5]. Observe that Endresen *et al.* consider C in the Farad unit (see Table 2 of [5]), while here C_m is a capacitance in $\mathrm{F.m}^{-2}$. Therefore C and $C_m \mathscr{A}(\Gamma)$ are homogeneous. Equation (14) is a generalization of the result of Endresen *et al.*

3 Numerical simulations

We perform numerical simulations of the linearized problem for the case of spherical cells. For all simulations, the initial radius equals 10μm. The numerical parameters are given in Table 2.

Observe that the constant $1/C_m$ is quite large since $C_m \sim 5.10^{-2}$ S.I. Therefore a steady-state is reached faster by the transmembrane potential than by the cell radius and the ionic concentrations. To solve the ordinary differential equations of the model we use the 4^{th} order Runge-Kutta scheme. This scheme has the advantage of being explicit (thus simple to implement) and at the same time quite stable compared with the usual Euler explicit scheme.

Table 2: Numerical parameters

R (gas constant)	8.3 J.K^{-1}.mol^{-1}
F (Faraday constant)	310 C.mol^{-1}
T (temperature)	310 K
r_0 (initial cell radius)	5.10^{-5} m
C_m (cell capacitance)	7.10^{-2}F.m^2
P_K (K^+ permeability)	4.10^{-10}m.s^{-1}
P_{Na} (Na^+ permeability)	$0.04P_K$
P_{Cl} (Cl^- permeability)	$3P_K$
P_X (permeability of non-permeant ions)	0
z_K (K^+ valency)	1
z_{Na} (Na^+ valency)	1
z_{Cl} (Cl^- valency)	-1
z_X^i (valency of non-permeant ions inside the cell)	-1.04
z_X^e (valency of non-permeant ions outside the cell)	-1.06

3.1 Effect of an osmotic stress on the transmembrane potential and the cell volume.

The value of τ_w is fixed at 10^{-12} s.m^{-1} as given by Landahl [16], which corresponds to a water permeability P_w of 10^{-5} m.s^{-1} (see Mathai *et al.* [20]). According to Lodish *et al.* [18], the inner and outer ionic concentrations for the mammalian cell in osmotic equilibrium are

$$[Na]_i = 12 \text{ mM}, \quad [K]_i = 139 \text{ mM}, \quad [Cl]_i = 4 \text{ mM}, \quad [X]_i = 141 \text{ mM}, \tag{15a}$$

$$[Na]_e = 145 \text{ mM}, \quad [K]_e = 4 \text{ mM}, \quad [Cl]_e = 116 \text{ mM}, \quad [X]_e = 31 \text{ mM}, \tag{15b}$$

and we imposed the values of the ions permeabilities and valencies given by Fraser and Huang [7] as[2]

$$P_K = 4.10^{-10} \text{ m.s}^{-1}, \quad P_{Na} = 0.04\, P_K, \quad P_{Cl} = 3\, P_K, \quad P_X = 0, \tag{15c}$$

$$z_{Na} = z_K = 1, \quad z_{Cl} = -1, \quad z_X^i = -1.04, \quad z_X^e = -1.06 \tag{15d}$$

For such concentrations, the resting transmembrane potential for a cell of radius $10\,\mu$m equals -88 mV[3]. We imposed this value as the initial condition for the transmembrane potential.

The simulations deal with the effect of an osmotic stress both on transmembrane potential and cell volume. The osmotic stress is applied at $t = 0$, and we let the system evolve. For the hypertonic trial, the outer osmotic pressure of the solution is set at 456 mM, while for the hypotonic trial, we increase the inner osmotic pressure to 456 mM. For both cases we investigate three types of

[2]The valencies z_X^i and z_X^e are the respective mean valencies of the non-permeant ions inside and outside the cell in order to ensure the electroneutrality of both outer and inner media. Since the non-permenant ions inside and outside the cell are different, then their respective mean valencies differ also.

[3]Observe that -88 mV is the resting membrane potential obtained by Fraser and Huang (Table 2 page 466 in [7]) for similar concentrations.

osmotic stresses: first we add non-permeant ions X^-, then study the effect of an increase in $NaCl$ concentrations and then do the same for KCl.

3.1.a Hyperosmotic stress

In order to study an hypertonic stress, we increase the outer osmolarity by 150 mM (from 296 mM to 446 mM). This stress is simulated in three ways: addition of non-permeant ions X ($[X]_e = 181$ mM), addition of $NaCl$ ($[Na]_e = 220$ mM, $[Cl]_e = 191$ mM), and addition of KCl ($[K]_e = 79$ mM, $[Cl]_e = 191$ mM), while the other concentrations remain unchanged. Fig. 1(b) gives the evolution of the cell volume for the three stresses. We observe the coincidence of the three curves, meaning that cell volume regulation is independent of the osmotic stress type.

The stabilization delay and change in volume obtained with the model correspond to experimental results presented by Ferenczi*et al.* (Fig 4.B, pp 429 [6]). On Fig. 1(a), we observe that the value of the transmembrane potential is highly dependent on the stress type. The value of the steady potential is around -90 mV when the stress is achieved by adding X ions or $NaCl$, whereas the potential changes dramatically and raises up to -50 mV when KCl is added. Stabilization of the transmembrane potential occurs within few seconds for the three stresses, while cell volume stabilization is achieved much later, as expected.

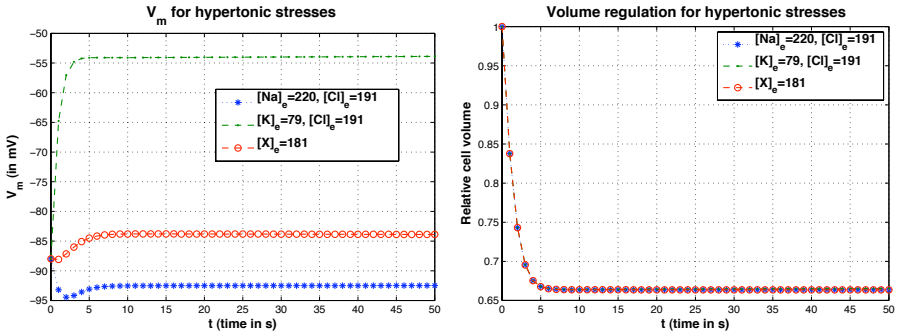

(a) Potential regulation (b) Volume regulation

Figure 1: Transmembrane potential (Fig. 1(a)) and cell volume (Fig. 1(b)) responses to a hypertonic stress: $P_e = 446$ mM, $P_i = 296$ mM. The water penetrability equals $\tau_w = 10^{-12}$ s.m^{-1}.

3.1.b Hypo-osmotic stress

We then study hypotonic stress, increasing the inner osmolarity by 150 mM (from 296 mM to 446 mM). Here again, the stress is simulated in three ways: addition of non-permeant ions X ($[X]_i = 291$ mM), addition of $NaCl$ ($[Na]_i = 87$ mM, $[Cl]_i = 79$ mM), and addition of KCl ($[K]_i = 219$ mM, $[Cl]_i = 74$ mM), other concentrations being unchanged. The evolution of the cell volume for the three stresses is displayed in Fig. 2(b). We observe that the three curves coincide, which means that the cell volume regulation is independent of the three types of osmotic stress, similarly to the hypertonic stresses. However,

the 3 minutes delay required for the cell volume stabilization is much larger than for the hypertonic trial. On Fig. 2(a), we observe that the value of the transmembrane potential is highly dependent on the stress type: it stabilizes around -30 mV when the stress is produced by addition of X ions or $NaCl$, whereas it dramatically lowers down to -90 mV with the addition of KCl. The transmembrane potential stabilizes within few seconds for the three stresses as for the hyperosmotic stresses.

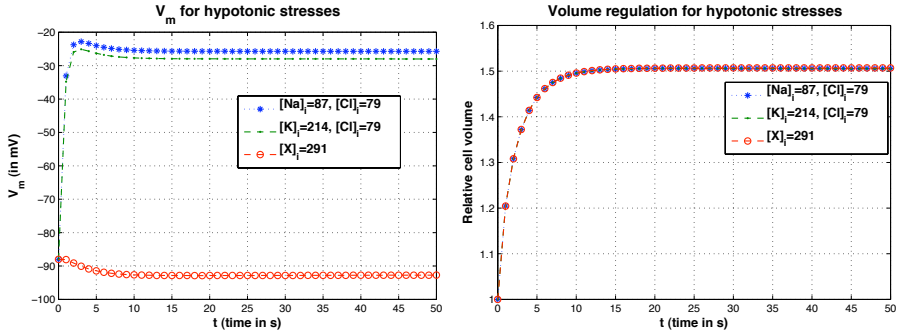

(a) Potential regulation (b) Volume regulation

Figure 2: Transmembrane potential (Fig. 2(a)) and cell volume (Fig. 2(b)) behaviours for hypertonic solution: $P_e = 296$ mM, $P_i = 446$ mM. The water penetrability equals $\tau_w = 10^{-12}$ s.m^{-1}.

3.1.c Influence of the coefficient τ_w on the dynamics

In this paragraph we study the effect of a reduction in water penetrability τ_w on the dynamics of the phenomena. Note the difference between the coefficient τ_w and the coefficient of permeability, since S.I. units for penetrability are s.m^{-1} and m.s^{-1} for permeability. The coefficient τ_w describes the time taken by a water molecule to cross the membrane: the higher τ_w, the more permeant the membrane is. In accordance with Landahl [16], τ_w usually equals 10^{-12} s.m^{-1}. We numerically investigate the effect of a reduction of this value. According to Fig. 3, when the membrane penetrability to water τ_w decreases from 10^{-12} s.m^{-1} to 10^{-14} s.m^{-1}, a delay in the stabilization of the cell volume can be observed. Actually, while the stabilization occurs in a few seconds for $\tau_w = 10^{-12}$ s.m^{-1}, the cell volume reaches its steady state within a minute when the value of τ_w decreases to 10^{-13} s.m^{-1} and no stabilization occurs before 4 min for $\tau_w = 10^{-14}$. Compared with the experiments of Rouzaire-Dubois *et al.* [21, 4, 22], the value of the stabilized cell volume is plausible. A decrease of τ_w, caused by alterations of the membrane phospholipids for instance, could explain the differences in the delays experimentally observed by Rouzaire-Dubois *et al.* [4, 21] in the cell osmotic stabilization. Moreover let us note that the values of the steady potential given by Fig. 4 are similar (around -90 mV) for τ_w equals 10^{-12}, 10^{-13} or 10^{-14}, meaning that a decrease of the penetrability of water does not affect the value of the transmembrane potential but dynamics of the volume regulation.

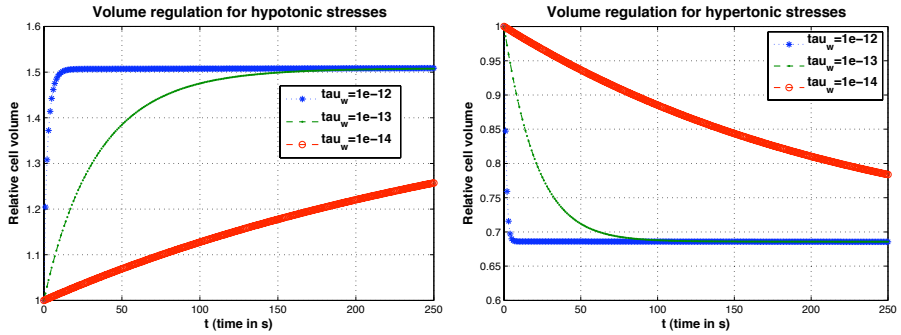

(a) Hypotonic stress (b) Hypoternic stress

Figure 3: Cell volume behaviour for hypotonic (Fig. 3(a)) and hypertonic (Fig. 3(b)) stresses of amplitude 150 mM by changing the concentration of non-permeant ions X.

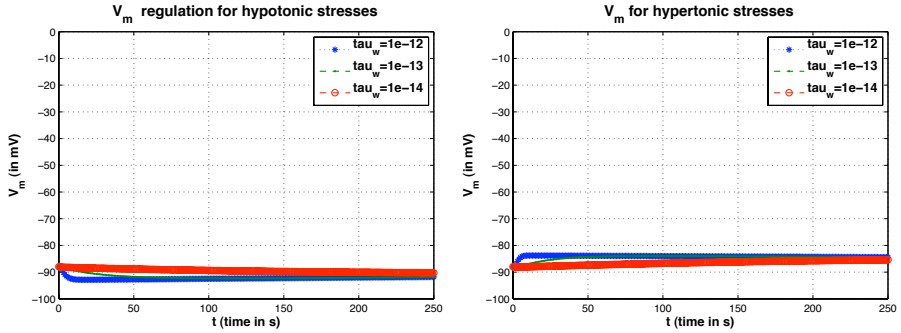

(a) Hypotonic stress (b) Hypertonic stress

Figure 4: Transmembrane potential behaviours for hypotonic (Fig. 4(a)) and hypertonic (Fig. 4(b)) stresses of amplitude 150 mM by changing the concentration of non-permeant ions X.

4 Preliminary experiments

In order to validate the theoretical results we performed preliminary experiments. More precisely in this section, we aim at showing that the dynamic of the experimental cell volume stabilization occurs within the time predicted by the model after osmotic stresses.

4.1 Materials and Methods

4.1.a Cell culture

DC-3F cells (Chinese hamster fibroblast lung cells) were grown in Minimum Essential Medium (Invitrogen, Cergy-Pontoise, France) supplemented with 10% fetal bovine serum (Invitrogen), 500 U/ml penicillin, 500 μg/ml streptomycin (Invitrogen) defined as complete medium. Cultures were maintained in a hu-

midified atmosphere with 5% CO_2 at 37°C. Cells were routinely passed every two days.

4.1.b Solutions used

The solutions used were all PBS based (D-PBS 10x, Invitrogen, diluted with milli-Q water, final molarities : Na^+ - 154 mM ; K^+ - 4 mM ; Cl^- - 140 mM ; $H_2PO_4^-$ - 1,5 mM ; HPO_4^{2-} - 8 mM). Hypertonic solutions were obtained by adding either $NaCl$ or KCl in order to increase their concentration by a minimum of 25 mM and a maximum of 300 mM.

4.1.c Fluorescence Activated Cell Sorter (FACS) experiments

Cells were harvested by trypsin and placed in a PBS solution for 15 minutes before any osmotic stress. The hypertonic stresses were obtained by adding the suitable volume of PBS supplemented with 300 mM $NaCl$ or KCl to 500 μL of the PBS containing the cells in suspension. In FACS analysis, forward scattering (FSC) was used to estimate the final volume ratios. Approximately 50.000 cells were run through the FACS three minutes after the hypertonic stresses. The measure lasted 40 s during which the FSC was stable. The dynamic evolution of the FSC was obtained starting with 800 μL of cells in suspension. 300 μL of those were used to obtain the initial FSC value. The tube was then removed from the FACS and replaced with another one containing the remaining 500μL mixed with the right volume of PBS supplemented with NaCl solution at 300 mM just before starting the stressed cells FACS acquisition. Each reported value is the average of 100 to 500 cells FSC acquisition.

4.2 Statistical analysis of FSC measurements

In static experiments, since the cells populations did not follow a Gaussian distribution, the mean FSC for each individual experiment is the average value of all the events considered as cells. Final results are the average of three individual experiments ± standard deviation (SD).

4.3 Results

For different hypertonic solutions, cells were analyzed using a FACS three minutes after the hypertonic stress. The mean FSC, which can be considered as a good representation of cells size, was measured and experimental volume ratios were thus calculated. Simultaneously numerical simulations of the model are performed with the experimental values of the initial concentrations. Experimental and numerical ratios are plotted on Fig. 5. It appears that theoretical values are very close to experimental data even though they are slightly under estimated for the hypertonic stress obtained by addition of KCl. Noticeably, for the same increase in molarity, the model predicts a lower amplitude of the volume change after KCl than $NaCl$ stress. Experimental data confirm this tendency but show a difference more important than the one predicted.

The dynamic evolution of the FSC (as explained in Materials and Methods) was recorded for the three different NaCl stresses indicated on Fig. 5. The experimental averaged data are plotted in thin line, the beginning of the stresses

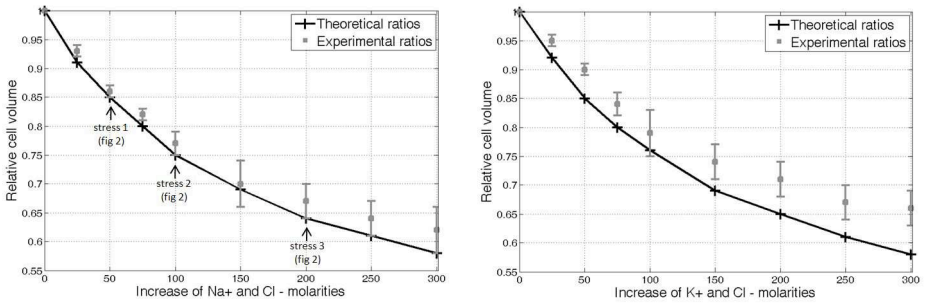

(a) Addition of $NaCl$ (b) Addition of KCl

Figure 5: Relative cell volume after stabilization for an osmotic stress of 150 mM by adding respectively $NaCl$ (Fig.5(a)) and KCl (Fig. 5(b)) (Means ± SD of three experiments).

being voluntarily shifted of ten seconds each. The part of the curves at no change in cell volume (initial FSC) were acquired from a 300 μL cell suspension. Then, the missing part of the curves corresponds to the time required for removing the tube from the FACS and replacing it with the cells just osmotically stressed. On Fig. 6 we have superimposed theoretical volume evolution for three different values of membrane penetrability to water denoted by τ_w. The experimental data provided by FSC cannot be precisely fitted since Fig. 5 shows that the final volume ratio values differed from the prediction. Still, we can give a good framing of τ_w as all three stresses have their best fit for $\tau_w = 7.10^{-13}$ s.m^{-1}. Stress 2 in particular validates the dynamic part of the model.

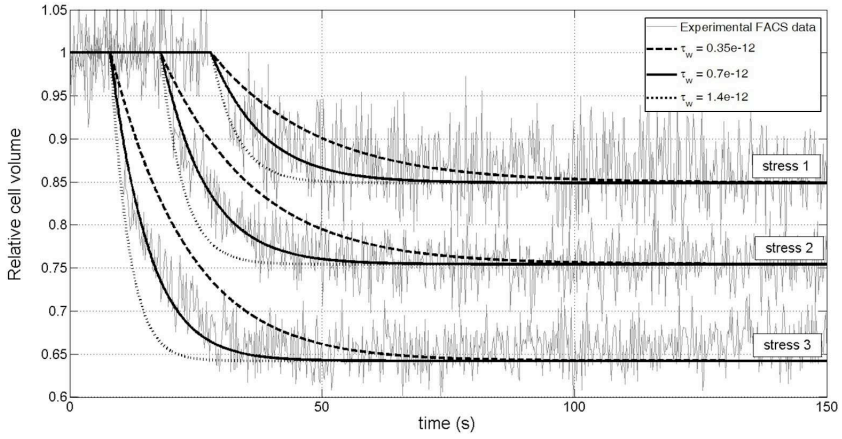

Figure 6: Dynamic evolution of the relative cell volume for the 3 stresses defined in the text.

5 Discussion

We have proposed a complete and generic model for the transmembrane potential and cell volume regulation. This model, based on ordinary differential equations, links dynamically the membrane potential, the cell volume, and the internal and external ionic concentrations. The main insight consists in taking into account the water diffusion across the membrane due to the osmotic pressure. This leads to an ordinary differential equation of the cell volume with respect to ionic concentrations. In the case of spherical cells, we explicitly link the behaviour of the cell volume to the transmembrane potential.

Preliminary experiments validate the model proposed in this manuscript. The numerical simulations fit very well with the experimental data after $NaCl$ addition, while a larger difference appears after KCl addition. It can be noticed that the final values obtained during dynamic experiments are coherent with the ones obtained by static analysis of a large number of cells. Moreover, the time resolution of the FACS seems well adapted to this kind of dynamics. Indeed, the FACS is fast enough to describe quite precisely the volume evolution, the time needed to actually mix solutions in order to make the stress being the limiting factor. FACS thus appears as an efficient tool to evaluate the volume evolution dynamically. In a next step it will be interesting to investigate if the dynamics are different depending on the cell types. Indeed the differences between KCl and $NaCl$ stresses might be relevant to metabolic issues. Using different cells types or acting on metabolism with appropriate drugs are avenues that appear worth exploring.

Our model can be derived to obtain the models presented previously by Jakobsson [14], Armstrong [1], Endresen *et al.* [5], Fraser and Huang [7], and Hernández [10]. More precisely, if the cell volume is constant, we recover the model of Endresen *et al.* [5], and if the osmotic equilibrium is instantly reached, our model is then similar to the model of Arsmtrong [1] and leads to the "Charge Difference" equation of Fraser and Huang [7]. However, these two hypotheses cannot explain the delays in cell volume stabilization experimentally observed by Rouzaire–Dubois *et al.* [4, 22] for the fifth generation of cells in culture submitted to a permanent osmotic stress. Comparatively, the first generation stabilizes very quickly [4]. Our model provides a possible explanation for such delays. Alterations of the membrane lipids, increasing with each new generation of cell culture, could decrease the value of τ_w, thus leading to such results.

6 Acknowledgements

The authors thank very warmly Professor O. Lafitte from the Department of Mathematics of Université Paris 13 for his well-considered advices and suggestions.

This research was partially supported by the INRIA collaborative research initiative ARC C3MB. A. Silve is supported by a DGA grant.

References

[1] C. M. Armstrong. The Na/K pump, Cl ion, and osmotic stabilization of cells. *P.N.A.S*, 100:6257–6262, 2003.

[2] T. Clausen and O.B. Nielsen. Potassium, na+,k+-pumps and fatigue in rat muscle. *J Physiol.*, 584:295–304, 2007.

[3] K. DeBruin and W. Krassowska. Modelling electroporation in a single cell. I. Effects of field strength and rest potential. *Biophysical Journal*, 77:1213–1224, Sept 1999.

[4] J-M. Dubois and B. Rouzaire-Dubois. The influence of cell volume changes on tumour cell proliferation. *Eur. J. Physiol.*, 33:227–232, 2004.

[5] L.P. Endresen, K. Hall, Høye J.S., and J. Myrheim. A theory of the membrane potential of living cells. *Eur. Biophys. J.*, 29:90:103, 2000.

[6] E. A. Ferenczi, J. A. Fraser, S. Chawla, J.N. Skepper, and C. Schwiening, C.J. Huang. Membrane potential stabilization in amphibian skeletal muscle fibres in hypertonic solutions. *J. Physiol.*, 555.2:423–438, 2003.

[7] J. A. Fraser and C. Huang. A quantitative analysis of cell volume and resting potential determination and regulation in excitable cells. *J. Physiol.*, 559.2:459–478, 2004.

[8] J. A. Fraser and C. Huang. Quantitative techniques for steady-state calculation and dynamic integrated modelling of membrane potential and intracellular ion concentrations. *Prog Biophys Mol Biol.*, 94:336–372, 2007.

[9] D.E. Goldman. Potential, impedance and rectification in membranes. *J. General Physiology*, 27:37–60, 1943.

[10] J.A. Hernández and E. Cristina. Modeling cell volume regulation in nonexcitable cells: the roles of the na+ pump and of cotransport systems. *Am. J. Physiol. Cell Physiol.*, 275:1067–1080, 1998.

[11] A.L Hodgkin and B. Katz. The effect of sodium ions on the electrical activity of the giant squid axon. *J.Physiology*, 108:37–77, 1949.

[12] L. Hodgkin and P. Horowicz. The influence of potassium and chloride ions on the membrane potential of single muscle fibres. *J. Physiol.*, 148:127–160, 1959.

[13] L. Hodgkin and A. Huxley. A quantitative description of membrane current and its application to conduction and excitation in nerve. *J. Physiol.*, 117:500–544, 1952.

[14] E. Jakobsson. Interactions of cell volume, membrane potential and membrane transport parameters. *American Journal of Physiology*, 238:C196–206, 1980.

[15] C. Juel. Potassium and sodium shifts during in vitro isometric muscle contraction, and the time course of the ion-gradient recovery. *PflugersArch.*, 406:458–463, 1986.

[16] H.D. Landahl. A note on the units of membrane permeability to water. *Bulletin of Mathematical Biophysics*, 10, 1948.

[17] F. Lang, G.L. Busch, M. Ritter, H. Völkl, S. Waldegger, E. Gulbins, and D. Häussinger. Functional significance of cell volume regulatory mechanisms. *Physiol Rev.*, 78:247–306, 1998.

[18] H. Lodish, A. Berk, L.S. Zipursky, P. Matsudaira, D. Baltimore, and Darnell J. *Molecular Cell Biology. Fourth Edition.* W.H. Freeman and company, New York, 1986.

[19] J. Malmivuo and R. Plonsey. *Bioelectromagnetism- Principles and Applications of Bioelectric and Biomagnetic Fields.* Oxford University Press, New York, 1995.

[20] J.C. Mathai, S. Tristram-Nagle, J.F. Nagle, and M.L. Zeidel. Structural determinants of water permeability through the lipid membrane. *The Journal of General Physiology*, 131(1):69–76, 2007.

[21] B. Rouzaire-Dubois and J-M. Dubois. K^+ channel block-induced mammalianthe influence of cell volume changes on tumour cell proliferation. *Eur. J. Physiol.*, 33:227–232, 2004.

[22] B. Rouzaire-Dubois, G. Ouanounou, S. O'Reagan, and J-M. Dubois. Sodium-dependent activity of aquaporin-1 in rat glioma cells: a new mechanism of cell volume regulation. *Eur. J. Physiol.*, 457:1187–1198, 2009.

[23] G. Sjøgaard, R.P. Adams, and B. Saltin. Water and ion shifts in skeletal muscle of humans with intense dynamic knee extension. *Am J Physiol.*, 248:190–196, 1985.

Centre de recherche INRIA Bordeaux – Sud Ouest
Domaine Universitaire - 351, cours de la Libération - 33405 Talence Cedex (France)

Centre de recherche INRIA Grenoble – Rhône-Alpes : 655, avenue de l'Europe - 38334 Montbonnot Saint-Ismier
Centre de recherche INRIA Lille – Nord Europe : Parc Scientifique de la Haute Borne - 40, avenue Halley - 59650 Villeneuve d'Ascq
Centre de recherche INRIA Nancy – Grand Est : LORIA, Technopôle de Nancy-Brabois - Campus scientifique
615, rue du Jardin Botanique - BP 101 - 54602 Villers-lès-Nancy Cedex
Centre de recherche INRIA Paris – Rocquencourt : Domaine de Voluceau - Rocquencourt - BP 105 - 78153 Le Chesnay Cedex
Centre de recherche INRIA Rennes – Bretagne Atlantique : IRISA, Campus universitaire de Beaulieu - 35042 Rennes Cedex
Centre de recherche INRIA Saclay – Île-de-France : Parc Orsay Université - ZAC des Vignes : 4, rue Jacques Monod - 91893 Orsay Cedex
Centre de recherche INRIA Sophia Antipolis – Méditerranée : 2004, route des Lucioles - BP 93 - 06902 Sophia Antipolis Cedex

Éditeur
INRIA - Domaine de Voluceau - Rocquencourt, BP 105 - 78153 Le Chesnay Cedex (France)
http://www.inria.fr
ISSN 0249-6399